

An Explanation of Anomalous Dielectric Relaxation Properties of Poly(propylene glycol)

K. L. Ngai*

Naval Research Laboratory, Washington, D.C. 20375-5000

A. Schönhals and E. Schlosser

Centrum für Makromolekulare Chemie, O-1199 Berlin, Germany

Received January 28, 1992; Revised Manuscript Received May 21, 1992

ABSTRACT: Dielectric measurements on low molecular weight poly(propylene glycol) over a wide frequency window of about 10 decades show that the relaxation times of the segmental relaxation and the normal modes have different temperature dependences. The segmental relaxation time, τ_s^* , has a much stronger temperature dependence than that of the normal-mode relaxation time, τ_n^* . As temperature is decreased, the shorter τ_s^* increases much faster than τ_n^* , with a tendency of τ_s^* to encroach τ_n^* resulting in a reduction of the dielectric strength of the normal mode. These dielectric results are analogous to that shown in viscoelastic data obtained in low molecular weight polystyrene by Plazek and explained previously by the coupling model. The dielectric data are explained quantitatively here also by the coupling model. Moreover, the molecular weight dependence of the normal-mode relaxation time at constant temperature is found experimentally to be significantly stronger than that expected from Rouse dynamics. It is a consequence of couplings between chains caused by hydrogen bonding of the OH end groups in poly(propylene glycol) and is explained here in the framework of the coupling model.

Introduction

In recent years there has been a revived interest in the normal modes of chains in low molecular weight poly(propylene glycol) with $500 < M_n < 4000$ concerning the effects the hydrogen bondings between the end groups may have on their dynamical properties.¹⁻⁶ As has been well established in other low molecular weight (unentangled) polymers without the additional complication of hydrogen bonding, the normal modes of chains and their viscoelastic properties are in remarkably good agreement with the modified Rouse model for undiluted polymers.⁷ The dynamical hydrogen-bonding interactions between end groups of chains may modify the internal normal modes (i.e., the $p \geq 1$ Rouse modes) and the mode of center-of-mass diffusion (i.e., the $p = 0$ Rouse mode). Experimental investigations of melts and solutions of poly(propylene glycol) (PPG) by ultrasonic absorption,¹ nuclear magnetic resonance,² and self-diffusion measurements^{3,5} have found that beyond a "critical" molecular weight M_k the motions are slowed down and the self-diffusion coefficient D is reduced to assume an approximately M^{-2} dependence on molecular weight M instead of the M^{-1} dependence it has at lower molecular weights. These experimental data were interpreted qualitatively as due to "entanglements" between transient associates caused by hydrogen bonding of the end groups. The M^{-2} dependence of D observed for $M > M_k$ probably prompted the suggestion^{4,5} that as a result of these transient entanglements reptationlike motion⁸ sets in for times on the order of the lifetimes of the associates.

Schlosser and Schönhals⁶ have examined the same problem using dielectric spectroscopy. The study of segmental relaxation and normal modes in PPG by dielectric measurements was initiated a long time ago by Baur and Stockmayer.⁹ The monomer unit of PPG has a dipole moment with nonzero components parallel and perpendicular to the chain backbone. These nonzero components enable the study of both segmental motion and the chain normal modes by dielectric spectroscopy. The new measurements by Schlosser et al. are made over a frequency window of $10^{-5} < f < 10^5$ Hz, much wider than

previous measurements. From isothermal measurement of dielectric loss as a function of frequency, the segmental relaxation and the normal mode each exhibit a peak with peak frequencies f_s and f_n , respectively, with f_s being higher. The wide frequency window enables the observation of both peaks isothermally over a considerable temperature range. In this range the temperature dependences of f_s and f_n and the spectral shapes of the two peaks can be determined and compared with each other. Actually, two Havriliak-Negami¹⁰ functions

$$\epsilon^*(f) - \epsilon_\infty = \Delta\epsilon \{1 + (i2\pi f\tau)^\beta\}^{-\gamma} \quad (1)$$

are used⁶ to characterize separately the two processes. Here $\Delta\epsilon$ is the dielectric strength and τ a characteristic relaxation time of the relaxation process. The fractional exponents β and γ determine the shape of the relaxation function. The high-frequency dielectric constant ϵ_∞ is defined as the limit of the real part of $\epsilon^*(f)$ at high frequencies. The maximum peak frequency f_p , the dielectric strength $\Delta\epsilon$, and the two fractional exponents β and γ were determined as functions of temperature. The method used to extract the Havriliak-Negami parameters for two overlapping relaxation processes in a wide frequency range has been described before.¹¹

The temperature dependences of f_s and f_n are very different although both are well-fitted by the Vogel-Fulcher-Tammann-Hesse (VFTH) equation⁷

$$\log f = \log f_\infty - A/(T - T_0) \quad (2)$$

The VFTH parameters of both processes have been given in ref 6. The shift factors $a_s(T) \equiv f_s(T)/f_s(T_{\text{ref}})$ and $a_n(T) \equiv f_n(T)/f_n(T_{\text{ref}})$ defined using the same reference temperature T_{ref} for both processes clearly bring out the fact that f_s has a much stronger temperature dependence than f_n . At high temperatures $f_s \gg f_n$ and the two processes are well separated in frequency. When temperature is lowered, because f_s decreases more rapidly than f_n , their separation in frequency decreases as f_s approaches f_n . Starting at higher temperatures, the dielectric strength $\Delta\epsilon_n$ of the normal mode increases with decreasing temperature, although the increase is not exactly $1/T$. However, at low

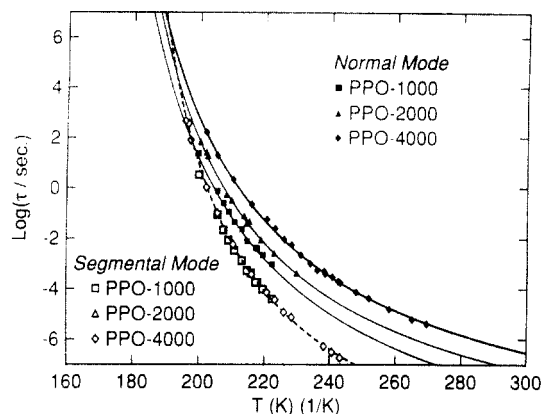


Figure 1. Temperature dependences of the segmental (S) relaxation time τ_s^* and the normal-mode relaxation time τ_2^* determined from dielectric relaxation measurements of PPG 1000 (\square, \blacksquare), PPG 2000 ($\triangle, \blacktriangle$), and PPG 4000 (\diamond, \blacklozenge) by Schlosser et al. The Vogel-Fulcher dependences as well as the actual data are plotted here. Encroachment of τ_s^* into the time domain of τ_2^* is evident.

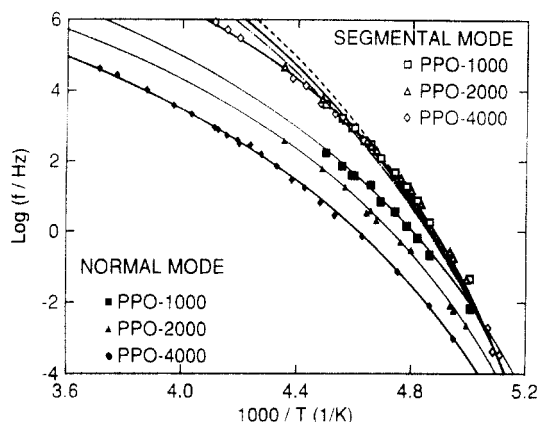


Figure 2. Frequency at the dielectric loss maximum plotted versus inverse temperature for the normal-mode process and the segmental relaxation. The points in this figure are the experimental data points, and the solid lines are from the Vogel-Fulcher equations of the segmental relaxation and the normal mode of PPG-1000, -2000, and -4000. It is clear that the segmental relaxation and the normal-mode process have different temperature dependences. The other lines are calculated by using eq 21 as explained in the text.

temperatures, where f_s is getting closer to f_n , the trend is reversed and $\Delta\epsilon_n$ instead decreases with decreasing temperature.

Schlosser et al.⁶ studied these dielectric properties as a function of molecular weight. Three PPG samples with molecular weights M_w of 1000, 2000, and 4000 were used to make the measurements. The segmental relaxation is independent of the molecular weight (see Figures 1 and 2). The same set of VFTH and HN parameters can be used to describe f_s and $\epsilon^*(f)$, respectively. The VFTH parameters of polymers with molecular weights M_w below the entanglement molecular weight M_c usually vary with M_w . Their independence of M_w for PPG is probably the consequence of hydrogen bondings between the OH end groups in PPG. On the other hand, the normal mode f_n at $T = 222$ K has a molecular weight dependence of

$$f_n \propto M^{-2.95} \quad (3)$$

which is significantly stronger than the

$$f_n \propto M^{-2} \quad (4)$$

dependence expected if the normal mode is governed by Rouse dynamics. In another polymer polyisoprene does

not have hydrogen bondings; the normal mode observed dielectrically¹² in samples with $M_w < M_c$ conforms to Rouse dynamics and the molecular weight dependence of eq 4. Hence, the deviation (eq 3) observed in PPG, like the M^{-2} dependence of D , is caused by hydrogen bonding. The trend of this deviation from Rouse dynamics is reflected in the shear viscosity data cited in ref 9. Although the viscosity data were taken at a considerably higher temperature regime, the viscosities, η , of the PPG liquids vary more rapidly than linearly with M expected from Rouse dynamics. The appropriate quantity to examine for molecular weight dependence and to compare with eq 3 is the shear viscoelastic relaxation time, τ_η , defined as the product ηJ_e where J_e is the recoverable compliance. Unfortunately information of J_e for the PPG liquids are not available, and quantitative comparisons between viscoelastic and dielectric data cannot be carried out at this time. It would be desirable in the future to have viscoelastic data of J_e and η in the same temperature range of dielectric measurements (Figures 1 and 2). In order to be absolutely sure that these deviations from Rouse dynamics are due only to H-bonding coupling, careful measurement of the PPG liquid density as a function of chain length is needed to rule out the remote possibility that the observed anomalous molecular weight dependences of the self-diffusion coefficient and normal-mode relaxation time are caused by a change of density with chain length.

In this work we address these various anomalous properties of both the segmental mode and the normal modes by the coupling model.¹³⁻¹⁸ Additional predictions will be made and compared with the dielectric data.

Coupling Model

The coupling model¹³⁻¹⁸ is based on fundamental and general physical principles to describe relaxation of a correlated or cooperative system in which the individual relaxing units are coupled with each other. It provides a solution to the problem of how the relaxation rates W_0 of individual units on the average are slowed down by interactions and correlations between the units. The rate slowing down has the form of $W(t) = W_0(\omega_c t)^{-n}$ where ω_c^{-1} is the onset time scale and $0 < n < 1$ is the coupling parameter. The parameters ω_c and n depend on the nature of the interactions although the form of $W(t)$ does not. The coupling model has been applied to segmental relaxation as well as normal-mode or terminal relaxation and self-diffusion. For segmental relaxation, intermolecular interactions between segments densely packed together in bulk polymers are responsible for the rate slowing down. Its coupling parameter n_s depends on the chemical structure of the monomer unit. For the normal modes and the self-diffusion mode in entangled monodisperse polymers, the intermolecular interactions are derived from chain entanglements and the coupling parameter, denoted here by n_n , is nonzero when $M_w \gtrsim M_c$. Here M_c is the molecular weight for entanglement. The PPG samples studied here are not entangled because $M_w < M_c$. However, an additional source of intermolecular interactions comes from hydrogen bondings between the end groups. Since the coupling model is based on fundamental physical principles, it is generally applicable to all correlated or coupled systems. In particular, it can be used to describe the dynamics of the normal modes in the presence of the hydrogen-bonding interactions. In the absence of the hydrogen-bonding interactions the normal modes should be well described by the Rouse model. As discussed by Baur and Stockmayer,⁹ PPG samples have two opposing sequences of longitudinal dipoles and the major contri-

bution to the dielectric spectrum comes from the second normal mode. Hence, we confine our attention to the $p = 2$ Rouse mode because it makes the dominant contribution to dielectric loss.^{9,16} The individual relaxation rate W_0 is then the reciprocal of the $p = 2$ Rouse relaxation time τ_2

$$\tau_2 = a^2 P^2 \zeta_0 / 24 \pi^2 k T \quad (5)$$

where a is a characteristic length, P the degree of polymerization, and ζ_0 the friction coefficient. The coupling parameter n_2 from hydrogen bonding for the $p = 2$ Rouse mode is not known a priori, but it can be deduced from the experimental data.

The prediction of the coupling model on the normal-mode contribution to the complex dielectric constant has been made before.¹⁷ This contribution has the frequency ($f = \omega/2\pi$) dependence of

$$\epsilon_n^*(\omega) - \epsilon_{n\infty} = \Delta\epsilon_n 8\pi^{-2} \int_0^\infty dt e^{-i\omega t} \left[-\frac{d}{dt} \exp[-(t/\tau_2^*)^{1-n_2}] \right] \quad (6)$$

where

$$\tau_2^* = \{(1 - n_2)\omega_c n_2 \tau_2\}^{1/(1-n_2)} \quad (7)$$

Equations 6 and 7 together with eq 5 spawn three simultaneous predictions from one and the same n_2 . They are as follows: (i) the shape of the $\epsilon_n^*(\omega)$ is determined by the Fourier transform of a Kohlrausch-Williams-Watts (KWW) function

$$\phi(t) = \exp[-(t/\tau_2^*)^\beta] \quad (8a)$$

where

$$\beta = 1 - n_2 \quad (8b)$$

if the sample is monodisperse and provided the small contribution to $\epsilon_n^*(\omega)$ from the higher Rouse modes can be dropped; (ii) the molecular weight dependence of the relaxation time τ_2^* , which is related to f_n^{-1} by a constant factor, is given by

$$\tau_2^* \propto M^{2/(1-n_2)} \quad (9)$$

if n_2 is independent of M ; and (iii) the temperature dependence of τ_2^* is given by

$$\tau_2^*(T) \propto [\zeta_0(T)/T]^{1/(1-n_2)} \quad (10)$$

Three different aspects of the experimental data, e.g., frequency, molecular weight, and temperature dependences, are predicted by three different relations involving the same n_2 . This means that the coupling parameter n_2 should not be regarded as an adjustable parameter because, by using one aspect of experimental data and comparing with the corresponding predicted relation, n_2 can be determined. This same value of n_2 so determined now offers two falsifiable predictions on the two remaining aspects of the experimental data.

If the polymer is polydisperse, then it is not practical to obtain the coupling parameter n_2 by fitting the Fourier transform of eq 8a to the experimental data of $\epsilon_n^*(\omega)$. The polydispersity will additionally broaden the dielectric loss peak. Even though eq 8a may still provide a good fit to the dielectric data, the value of β so determined will no longer be related to the coupling parameter n_2 via eq 8b.¹⁶ Only when dealing with near monodisperse samples as in the case of polyisoprenes¹⁸ will this method of determining n_2 be directly applicable.

The molecular weight dependence of f_n is known from experiments and given by eq 3. Let us assume that the

coupling parameter of the $p = 0$ Rouse mode has the same value as n_2 in the present case where intermolecular interactions are the hydrogen bondings. It follows from eq 7 that τ_0^* and τ_2^* will have the same molecular weight dependence, and accordingly the self-diffusion coefficient will have the molecular weight dependence given by

$$D \propto \langle R_g^2 \rangle / \tau_0^* \propto \langle R_g^2 \rangle / \tau_2^* \propto M^{-1.95} \quad (11)$$

This is in good agreement with $D \propto M^{-2}$ determined by NMR pulsed field gradient technique⁵ and dynamic light scattering. Thus the molecular weight dependence

$$\tau_2^* \propto M^{2.95}$$

is a reliable result. Our strategy is to use this aspect of the dielectric data, compare with the corresponding predicted eq 9, and determine n_2 in the process. The value we find is

$$n_2 = 0.32 \quad (12)$$

With n_2 determined, the frequency dependence of the contribution of the normal mode to the complex dielectric constant is predicted to be given by eqs 6 and 8a,b. Experimentally, the data of the normal-mode contribution have been fitted with the four-parameter Havriliak-Negami (HN) empirical equation. From the connection between the HN and the KWW functions, the same data if fitted by the KWW function require¹⁹

$$\beta = 0.615 \quad (13)$$

Only data taken at higher temperatures (higher frequencies) are used in the determination of the KWW exponent because at lower temperatures the segmental relaxation time τ_s^* approaches τ_2^* (Figure 1). The separation of the two contributions becomes more difficult, and the β value determined is less reliable. The β value found, from eq 8b, corresponds to

$$n = 0.385 \quad (14)$$

which is larger than the theoretical value of 0.32 given by eq 12. The discrepancy found is consistent with the slight polydispersity of the PPG samples used which has the effect of broadening the dielectric loss peak.¹⁶ The discrepancy is small and in the right direction as expected from additional broadening caused by polydispersity of the samples used, $M_w/M_n < 1.2$.

The third aspect of the experimental data that can be compared with prediction as given by eq 10 is the temperature dependence of τ_2^* . We shall return to this comparison after a brief discussion of the properties of segmental relaxation. The segmental motion makes another contribution to the complex dielectric constant which according to the coupling model is given by²⁰

$$\epsilon_s^*(\omega) - \epsilon_{s\infty} = \Delta\epsilon_s \int_0^\infty dt e^{-i\omega t} \left[-\frac{d}{dt} \exp[-(t/\tau_s^*)^{1-n_s}] \right] \quad (15)$$

Here n_s is the coupling parameter for segmental motion and the relaxation time τ_s^* is related to the single-chain conformation²¹ relaxation time τ_s by the relation

$$\tau_s^* = \{(1 - n_s)\omega_c n_s \tau_s\}^{1/(1-n_s)} \quad (16)$$

The temperature dependence of τ_s is governed by the same friction factor $\zeta_0(T)$ that appears in eqs 5 and 10. The temperature dependence of τ_s^* accordingly is

$$\tau_s^*(T) \propto [\zeta_0(T)]^{1/(1-n_s)} \quad (17)$$

The value of the segmental relaxation coupling parameter, n_s , depends on the strength of the intermolecular inter-

actions and hence on the structure of the repeat unit. By examining segmental relaxation in many amorphous polymers,²² a correlation between the temperature dependence of τ_s^* and the coupling parameter n_s as implied by eq 17 has been verified. For PPG, dielectric data of previous measurements and recent measurement by Schlosser et al.⁶ can be fitted by the KWW function as indicated by eq 15. The fit determines the coupling parameter, and its value is

$$n_s = 0.50 \quad (18)$$

With any arbitrary choice of a reference temperature, T_{ref} , the temperature dependences given by eqs 10 and 17 can be expressed as shift factors

$$a_2(T) \equiv \tau_2^*(T)/\tau_2^*(T_{\text{ref}}) = [\zeta_0(T)T_{\text{ref}}/\zeta_0(T_{\text{ref}})T]^{1/(1-n_2)} \quad (19)$$

and

$$a_s(T) = \tau_s^*(T)/\tau_s^*(T_{\text{ref}}) = [\zeta_0(T)/\zeta_0(T_{\text{ref}})]^{1/(1-n_s)} \quad (20)$$

We can relate $a_s(T)$ to $a_2(T)$ as

$$\log a_s(T) = \left[\frac{(1-n_2)}{(1-n_s)} \right] \log a_2(T) - \frac{1}{1-n_s} \log (T_{\text{ref}}/T) \quad (21)$$

The peak frequencies f_s and f_n are inversely proportional to τ_s^* and τ_2^* , respectively. Hence, their temperature dependences are determined by

$$\log f_s(T) = \log f_s(T_{\text{ref}}) - \log a_s(T) \quad (22)$$

and

$$\log f_n(T) = \log f_n(T_{\text{ref}}) - \log a_2(T) \quad (23)$$

The comparison between the temperature dependence of $\tau_2^*(T)$ obtained from experiment with the coupling model prediction directly through eq 10 is not possible because $\zeta_0(T)$ has not been determined explicitly. However, taking advantage of the fact from eq 17 that $\tau_s^*(T)$ is related also to $\zeta_0(T)$, we can eliminate $\zeta_0(T)$ in favor of $\tau_s^*(T)$. The coupling model predicts a relation (eq 21) between the shift factors of τ_2^* and τ_s^* that is parameterless because earlier n_2 and n_s have been determined by other aspects of the experimental data. Since $\tau_2^*(T)$ and $\tau_s^*(T)$ have been measured and their shift factors $a_2(T)$ and $a_s(T)$ determined, the predicted relation between them is parameterless and offers a stringent test of the model.

The method used to test this prediction is described as follows: We start with the experimental data of $f_n(T)$ and its VFTH expression obtained from the good fit to the experimental data points. An arbitrary T_{ref} within the temperature range of experimental measurements is chosen, and the values of the two known quantities $f_s(T_{\text{ref}})$ and $f_n(T_{\text{ref}})$ are noted. The shift factor $a_2(T)$ is then determined as a function of T . The shift factor of segmental motion $a_s(T)$ is calculated by using eq 21 where the coupling parameters n_2 and n_s have been determined previously (see eqs 12 and 18). Finally we use eq 22 to calculate $f_s(T)$. The critical test of the prediction is shown in Figure 2 where we compare the calculated $f_s(T)$ with the experimental $f_s(T)$ represented here by the VFTH fit to the actual experimental points. To calculate $f_s(T)$, we take the Vogel-Fulcher equation

$$\log f_n = 10.1 - 643/(T - 153) \quad (24)$$

for the normal mode of PPG-4000,⁶ deduce its the shift factor $a_2(\tau)$, scale $\log a_2(T)$ by the factor $(1-n_2)/(1-n_s)$, and obtain $f_s(T)$ from eqs 21 and 22. The results shown

as the dashed curve in Figure 2 provide a reasonably good fit to the experimental data particularly at lower temperatures. Other choices of the coupling parameters allowed within their experimental error give better fits to the experimental data at higher temperatures. The results for these choices are illustrated in Figure 2 for the pair $n_s = 0.49$ and $n_2 = 0.34$ (solid curve) and for the pair $n_s = 0.48$ and $n_2 = 0.35$ (dash-dotted curve). There is good overall agreement between experiment and theory, and we may conclude that the predictions on the temperature dependences (eqs 10 and 17) are also verified. The situation is similar for the other PPG samples with different molecular weights.

Time-Scale Encroachment

Equation 21, when written out explicitly and neglecting the small term, has the form

$$\log a_s(T) = 1.39 \log a_2(T) \quad (25)$$

This result of the coupling model indicates that the two shift factors are not the same. The logarithm of the shift factor of segmental relaxation is about 40% larger than that of the normal mode. Such a large difference between the two shift factors from dielectric measurements is consistent with recoverable creep compliance data obtained earlier by Cochrane et al.²³

A large difference between the shift factor of segmental motion and the shift factor $a_0(T)$ for the Rousean diffusion mode was observed in another low molecular weight amorphous polymer poly(phenylmethylsiloxane) (PPMS) by dynamic light scattering.¹⁶ In this study the PPMS sample has a molecular weight of 2500 and is unentangled. There are no hydrogen-bonding interactions in PPMS, and the coupling parameter n_0 for the $p = 0$ normal mode vanishes. Instead of eq 21, the relation

$$\log a_s(T) = \frac{1}{1-n_s} \log a_0(T) \quad (26)$$

follows from the coupling model. This relation was verified by the dynamic light scattering data.¹⁵ At high molecular weights, entanglement couplings between chains make the coupling parameter for the $p = 1$ Rouse mode, n_1 , nonzero. For monodisperse linear polymers, n_1 has the value^{13,14} of approximately 0.41. The relations given by eqs 25 and 26 are replaced by

$$\log a_s(T) = \frac{1-0.41}{1-n_s} \log a_1(T) \quad (27)$$

where $a_1(T)$ is the shift factor for the $p = 1$ mode. Again this relation was verified by viscoelastic data of polystyrene, poly(vinyl acetate),^{14,24} and atactic polypropylene.²⁵ The successes the coupling model has in predicting the relation between the two shift factors under various conditions including the present case of PPG are noteworthy.

The segmental relaxation time is usually much shorter than the normal-mode relaxation time. Experimentally this is in fact the case at higher temperatures (Figure 1). However, because of eq 25, the separation in the time scale between τ_s^* and τ_2^* decreases continuously as temperature is reduced. As a result τ_s^* encroaches into the time domain of τ_2^* as observed in the dielectric measurements. This encroachment leads to an observable consequence on the dielectric strength of the normal mode to be discussed next.

Loss of Normal Modes

On decreasing temperature, when encroachment of τ_s^* makes the separation between τ_2^* and τ_2^* too small, the

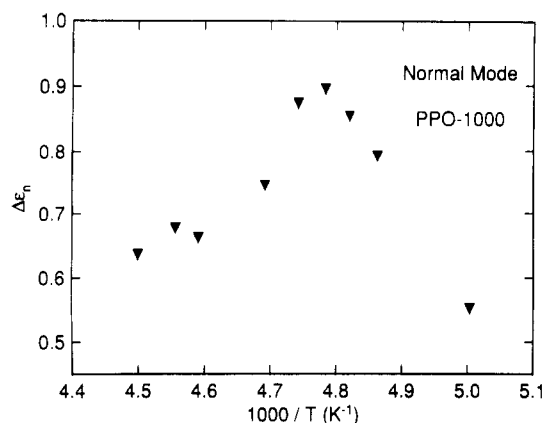


Figure 3. Temperature dependence of the intensity $\Delta\epsilon_n$ of the normal-mode process of PPG-1000.

longest wavelength normal mode becomes the first to be arrested and ceases to contribute to viscoelasticity and dielectric relaxation. A qualitative theory of the loss of normal modes based on the encroachment of τ_s^* toward τ_2^* in low molecular weight polymers was given in ref 26. This theoretical explanation is applicable to the dielectric data of PPG obviously because encroachment is indeed observed in Figure 1. The predicted loss of the normal-mode contribution is also observed. In Figure 3 the measured intensity or dielectric strength $\Delta\epsilon_n$ of the normal mode is plotted against $1/T$. Instead of a monotonic increase expected from a $1/T$ dependence of $\Delta\epsilon_n$, we find a precipitous drop at the low-temperature end. This precipitous drop of $\Delta\epsilon_n$ is consistent with the loss of the contribution from the normal mode due to its arrest caused by encroachment of τ_s^* and in agreement with the mechanical recoverable compliance measurements.^{23,24,26,27}

Summary and Discussion

The presence of hydrogen bonding between the end groups introduces a new form of intermolecular interactions in unentangled low molecular weight PPG. The effects of these intermolecular interactions on the dynamics of the normal modes are considered in the framework of the coupling model. Predictions that touch upon three different aspects of the experimental data are made and shown to be in good agreement with measurements. As demonstrated before the coupling model is also applicable to the dynamics of the segmental relaxation. The breakdown of thermorheological simplicity, with the segmental relaxation time having a much stronger temperature dependence than that of the normal modes, can be explained on a quantitative basis. The encroachment of the segmental relaxation time into the time domain of the normal modes as temperature decreases and its consequence (a precipitous drop in the dielectric intensity $\Delta\epsilon_n$) are expected from the coupling model. These expected properties are seen experimentally in the dielectric data.

Suggestions have been made that the dynamics of the normal modes in PPG may be explained by the formation of associates or transient entanglements and reptationlike motion for times of the order of the lifetimes of the associates. This explanation can explain the $D \propto M^{-2}$ dependence of the self-diffusion coefficient and the $\tau_n^* \propto M^{2.95}$ dependence of the dielectric normal-mode relaxation time. However, it cannot explain the dielectric dispersion (i.e., frequency dependence) of the normal mode having the KWW form with the stretch exponent given by eq 13 and the relaxation time having a temperature dependence much weaker than that of the segmental relaxation.

Moreover, it cannot explain the encroachment of the segmental relaxation time and the precipitous drop of $\Delta\epsilon_n$ on lowering temperature. On the other hand, the coupling model explains all these features of the experimental data of PPG as well as similar or related experimental data of other low molecular weight polymers without hydrogen-bonding interactions and high molecular weight entangled linear polymers. Some readers, though impressed with the good description of the segmental and normal-mode processes here by the coupling model, may like to see more physical arguments for the reason why the coupling model applies so well. Such physical arguments ultimately will come from the theory behind the model itself. We believe that the recent theoretical development of the coupling model based on interacting chaotic Hamiltonian dynamics¹⁸ and further refinements expected in the future will shed more light on the physics of relaxation of correlated systems of which segmental and normal-mode processes in PPG are just special cases.

References and Notes

- Alig, I.; Grigorev, S. B.; Manucarov, Yu. S.; Manucarova, S. A. *Acta Polym.* **1986**, *37*, 689, 733.
- Alig, I.; Donth, E.; Schenk, W.; Höring, S.; Wohlfarth, Ch. *Polymer* **1988**, *29*, 2081.
- Zgadzai, O. E.; Skirda, V. D.; Maklakov, A. I.; Chalych, A. E. *Dokl. Akad. Nauk SSSR* **1987**, *297*, 1407.
- Heinrich, G.; Alig, I.; Donth, E. *Polymer* **1988**, *29*, 1189.
- Fleischer, G.; Helmstedt, M.; Alig, I. *Polym. Commun.* **1990**, *31*, 409.
- Schlosser, E.; Schönhals, A. *Colloid Polym. Sci.*, in press.
- Schlosser, E.; Schönhals, A., to be submitted for publication in *Polym. Commun.*
- Ferry, J. D. *Viscoelastic Properties of Polymers*; John Wiley: New York, 1980.
- de Gennes, P.-G. *Scaling Concepts in Polymer Physics*; Cornell University Press: Ithaca, NY, 1979.
- Baur, M. E.; Stockmayer, W. H. *J. Chem. Phys.* **1965**, *43*, 4319.
- Havriliak, S.; Negami, S. *J. Polym. Sci., Polym. Symp.* **1966**, *14*, 89.
- Schlosser, E.; Schönhals, A. *Colloid Polym. Sci.* **1989**, *267*, 963.
- Boese, D.; Kremer, F. *Macromolecules* **1990**, *23*, 829.
- Kremer, F.; Boese, D.; Fetters, L. J. *Non-Cryst. Solids* **1991**, *131-133*, 728.
- Schönhals, A., to be published in *J. Non-Cryst. Solids*.
- For a review see: Ngai, K. L.; Rendell, R. W.; Rajagopal, A. K.; Teitler, S. *Ann. N.Y. Acad. Sci.* **1986**, *484*, 150.
- Ngai, K. L.; Plazek, D. J. *J. Polym. Sci., Polym. Phys. Ed.* **1986**, *24*, 619 and references therein.
- McKenna, G. B.; Ngai, K. L.; Plazek, D. J. *Polymer* **1985**, *26*, 165.
- Ngai, K. L.; Fytas, G. *J. Polym. Sci., Polym. Phys. Ed.* **1986**, *24*, 1683.
- Ngai, K. L.; Rendell, R. W. *Macromolecules* **1987**, *20*, 1066.
- For recent versions of the coupling model based on classical chaos, see: Ngai, K. L.; Rendell, R. W. *J. Non-Cryst. Solids* **1991**, *131-133*, 233.
- Peng, S. L.; Ngai, K. L.; Tsang, K. Y., to be published in *J. Non-Cryst. Solids*.
- Alvarez, F.; Alegria, A.; Colmenero, J. *Phys. Rev.* **1991**, *B44*, 7306.
- Ngai, K. L. In *Non-Debye Relaxations in Condensed Matter*; Ramakrishnan, T. V.; Raj Lakshmi, M., Eds.; World Scientific: Singapore, 1987; p 23.
- Ngai, K. L.; Rendell, R. W. *J. Non-Cryst. Solids* **1991**, *131-133*, 942.
- Plazek, D. J.; Ngai, K. L. *Macromolecules* **1991**, *24*, 1222.
- Cochrane, J.; Harrison, G.; Lamb, J.; Phillips, D. W. *Polymer* **1980**, *21*, 2049.
- Plazek, D. J. *J. Non-Cryst. Solids* **1991**, *131-133*, 836.
- Fytas, G.; Ngai, K. L. *Macromolecules* **1988**, *21*, 804.
- Ngai, K. L.; Plazek, D. J.; Deo, S. S. *Macromolecules* **1987**, *20*, 3047.
- Ngai, K. L.; Plazek, D. J., to be published in *Macromolecules*.
- Plazek, D. J.; O'Rourke, V. M. *J. Polym. Sci.* **1971**, *A29*, 209.